OBSERVATIONS ON THE FINE STRUCTURE AND CYTOCHEMISTRY OF MOUSE AND HUMAN INTERCOSTAL NEUROMUSCULAR JUNCTIONS

S. I. ZACKS, M.D., and J. M. BLUMBERG, M.D.

From the Armed Forces Institute of Pathology, Washington, D. C.
Dr. Zacks' present address is Ayer Clinical Laboratory, Pennsylvania Hospital, Philadelphia

ABSTRACT

The fine structure of the mouse and human intercostal muscle neuromuscular junction was studied after brief fixation in a new formol-sucrose fixative. This primary formalin fixation was followed by brief postosmication in buffered 1 per cent osmium tetroxide. Muscle blocks were embedded in methacrylate or Epon 812 epoxy resin. Marked similarities between mouse and human motor end-plates were observed. Neuromuscular junctions from both mouse and human intercostal muscle showed synaptic vesicles, primary and secondary synaptic clefts, and layered differentiation of the amorphous surface material (ASM) present on the surface of the Schwann cell plasma membrane and on the muscle surface membrane in the region of the neuromuscular junction. An attempt to stain the ASM with lead was unsuccessful. Observations on thick and thin plastic-embedded sections stained by PAS after diastase digestion showed that the ASM within the subneural apparatus is PAS positive. Alcian blue stained the endoneurium and perineurium of peripheral nerve bundles and portions of the end-plates. The similarity of the PAS-positive ASM to other basement membranes described in other sites is discussed and its possible physiologic significance within the subsynaptic apparatus is considered.

Several electron microscope studies of the fine structure of neuromuscular junctions in laboratory animals have been reported in recent years (1, 4, 13, 34, 36, 37). Only recently has a study concerning human motor end-plates appeared (13). In general, the published investigations agree on many common features of the neuromuscular junction, including the presence of primary and secondary synaptic clefts, synaptic vesicles, axoplasmic and sole-plate mitochondria, and aposynaptic granules. The major point of disagreement among the several investigators concerns the structure of the material filling the space between the axolemma and the sarcolemma. It has been described as membranous and five layered (36), three layered (37), or completely amorphous (1, 13).

The present investigation was undertaken to attempt to obtain information concerning the comparative fine structure and cytochemistry of mouse and human neuromuscular junctions, especially with respect to the "ground substance" within the subsynaptic apparatus. It was hoped that this information would facilitate interpretation of possible alterations in experimentally altered and pathologic neuromuscular junctions.

MATERIALS AND METHODS

Mice were killed by a blow on the head and the thorax was rapidly excised and was placed immediately in freshly prepared formol-sucrose fixative (41). After fixation for 15 to 20 minutes at 4°C or room temperature, the hemithorax was washed briefly in veronal-sucrose buffer (pH 7.35). Thin strips of

intercostal muscle were cut from the ribs and divided into 0.5 mm blocks, which were placed in buffered 1 per cent osmium tetroxide for 7 to 15 minutes. These blocks were washed in veronal-sucrose buffer, rapidly dehydrated in graded ethanol, and embedded in a mixture of 30 per cent methyl and 70 per cent butyl methacrylate which had been dried with Drierite and silica gel. Two per cent Luperco accelerator and uranyl nitrate (15 mg/ml) (39) were added to the dried methacrylate. The plastic was allowed to polymerize overnight at 60°C.

Thick sections were cut on a Porter-Blum microtome with glass knives. The methacrylate was removed from the thick (0.5 μ) sections with carbon tetrachloride followed by xylene, mounted in 1.460 immersion oil (12, 29), and examined by oil-immersion phase microscopy. Innervation sites were selected in this way, and the blocks were trimmed for thin sectioning. Silver sections were examined in an RCA EMU-3D electron microscope equipped with a 1 mil objective aperture. Other blocks were embedded in Epon 812[1] according to the method of Luft (24).

Human intercostal muscle biopsies were obtained from patients subjected to thoracotomy for repair of acquired or congenital cardiac defects or for thoracic exploration. General anesthesia without neuromuscular blocking agents was used. Small fragments (2 $\times$ 0.5 $\times$ 0.5 cm) of muscle were taken from the pleural surface at the time of primary intercostal muscle incision without methylene blue staining or electrode recording of end-plate potentials. The muscle blocks were fixed immediately in freshly prepared formol-sucrose solution. Neuromuscular junctions from both adults and children were studied.

Cytochemical Methods

Staining with PAS and Alcian Blue: Mouse and human intercostal muscle was fixed in formol-sucrose solution, embedded in paraffin, sectioned at 6 μ and stained by the PAS method of McManus (25). Fragments of sucrose-formalin-fixed muscle were stained by the PAS method, cleared, and prepared as whole mounts for the study of nerve motor end-plate rela-

---

[1] Trademark, Shell Chemicals, New York.

tionships. Control preparations were treated with malt diastase to remove glycogen.

Mouse and human muscle fixed in sucrose-formalin was also stained by the following methods: PAS-Alcian blue (27), Bodian (19), Bielschowsky (19), and hematoxylin and eosin.

The PAS method was modified to permit study of 0.5 to 2 μ sections embedded in methacrylate or Epon 812. Sections 0.5 to 2 μ thick were cut on the Porter-Blum microtome with glass knives and dried on slides. The methacrylate was removed by immersion in carbon tetrachloride for 5 minutes followed by rinsing in xylene. The sections were mounted in immersion oil of 1.460 refractive index and examined by oil-immersion phase microscopy. After end-plate-rich areas had been located and their coordinates recorded from a graduated mechanical stage, the immersion oil was removed with xylene. The slides were then rehydrated through decreasing concentrations of ethanol. After thorough rinsing in distilled water, the sections were incubated with malt diastase (0.5 per cent) at 37°C for 30 minutes. The sections were again washed and exposed to 0.5 per cent periodic acid for 10 minutes. The acid was washed from the sections, and they were stained with "cold Schiff" (19) reagent for 10 to 15 minutes. Three sodium acid sulfite rinses, followed by washing in running tap water, completed the staining procedure. To facilitate identification of muscle and sole-plate nuclei, the sections were counterstained with Mayer hemalum (with acetic acid) for 5 minutes. Differentiation in dilute acetic acid, washing, dehydration, and mounting were the final steps in the procedure. *Lead Staining:* Freshly excised blocks of intercostal muscle were placed in barbital-buffered (pH 7.35) solutions of Pb(NO₃)₂ (50 mg/ml) for 20 minutes (38), fixed in formol-sucrose, postosmicated for 10 minutes in 1 per cent buffered (pH 7.35) osmium tetroxide, and embedded for electron microscopy.

OBSERVATIONS

Electron Microscopy

Mouse Neuromuscular Junctions: Over fifty mouse intercostal neuromuscular junctions were studied

---

Key to Abbreviations in Figures

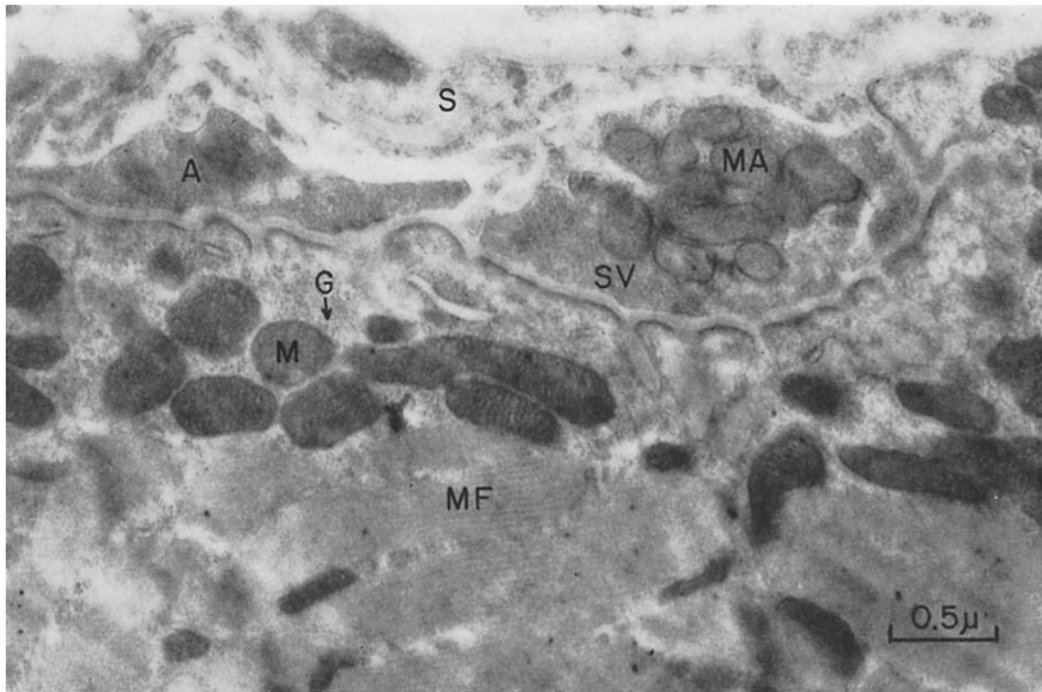|	
A, axon	N, nucleus
AC, axis cylinder	PSC, primary synaptic cleft
ASM, amorphous surface material	R, endoplasmic reticulum
C, capillary	S, Schwann cell
G, aposynaptic granules	SA, subsynaptic apparatus
M, mitochondria	SSC, secondary synaptic cleft
MA, mitochondria of axon	SV, synaptic vesicle
MF, muscle fiber	V, vesicle

Figure 1

Electron micrograph of mouse intercostal neuromuscular junction showing relationship of terminal axon branches to the subsynaptic apparatus. Epon embedded. × 14,500.
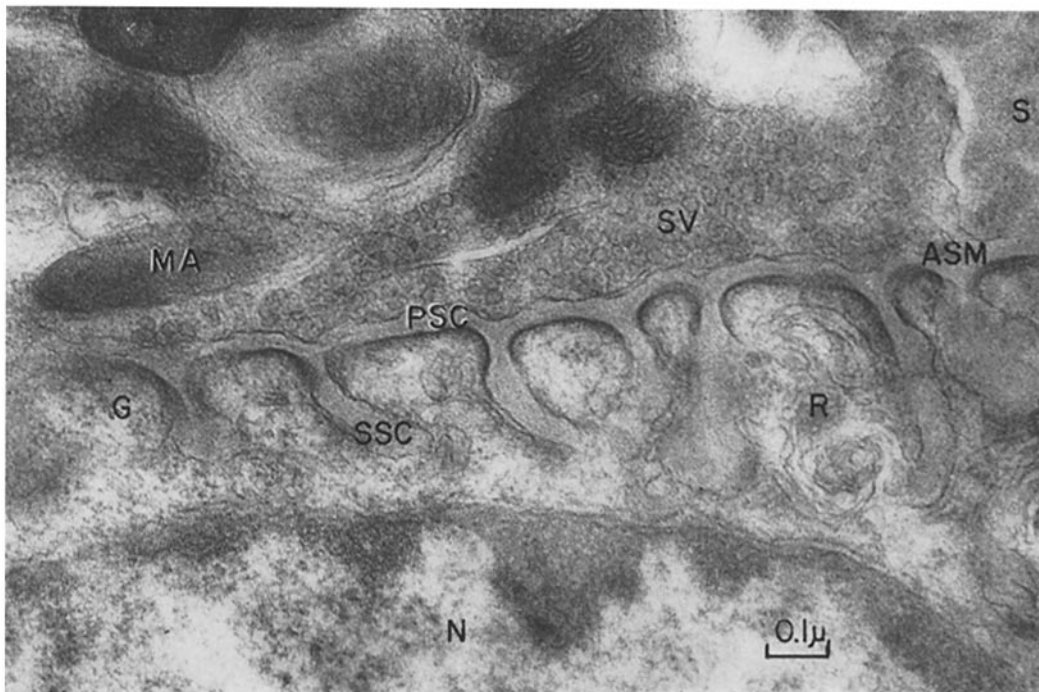

Figure 2

Electron micrograph of mouse intercostal neuromuscular junction showing details of the synaptic vesicles and primary and secondary synaptic clefts. Note the layers of ASM with the secondary clefts. Epon embedded. × 80,000.

in material embedded in methacrylate or Epon 812.

The mouse intercostal end-plates measured 40 to 50 μ in width and approximately 3 μ in thickness. They were composed of several terminal axon branches that lay in depressions in the sarcoplasmic surface (Figs. 1 and 2). Accumulations of mitochondria were noted beneath the muscle surface membrane in the sole-plate area, and prominent capillaries were intimately related to the innervation sites. Overlying the terminal axon branches, and intimately related to the axon membrane, was a mass of Schwann cell cytoplasm that occasionally showed complex infoldings with the axon surface membrane. The Schwann cell cytoplasm and nucleus showed
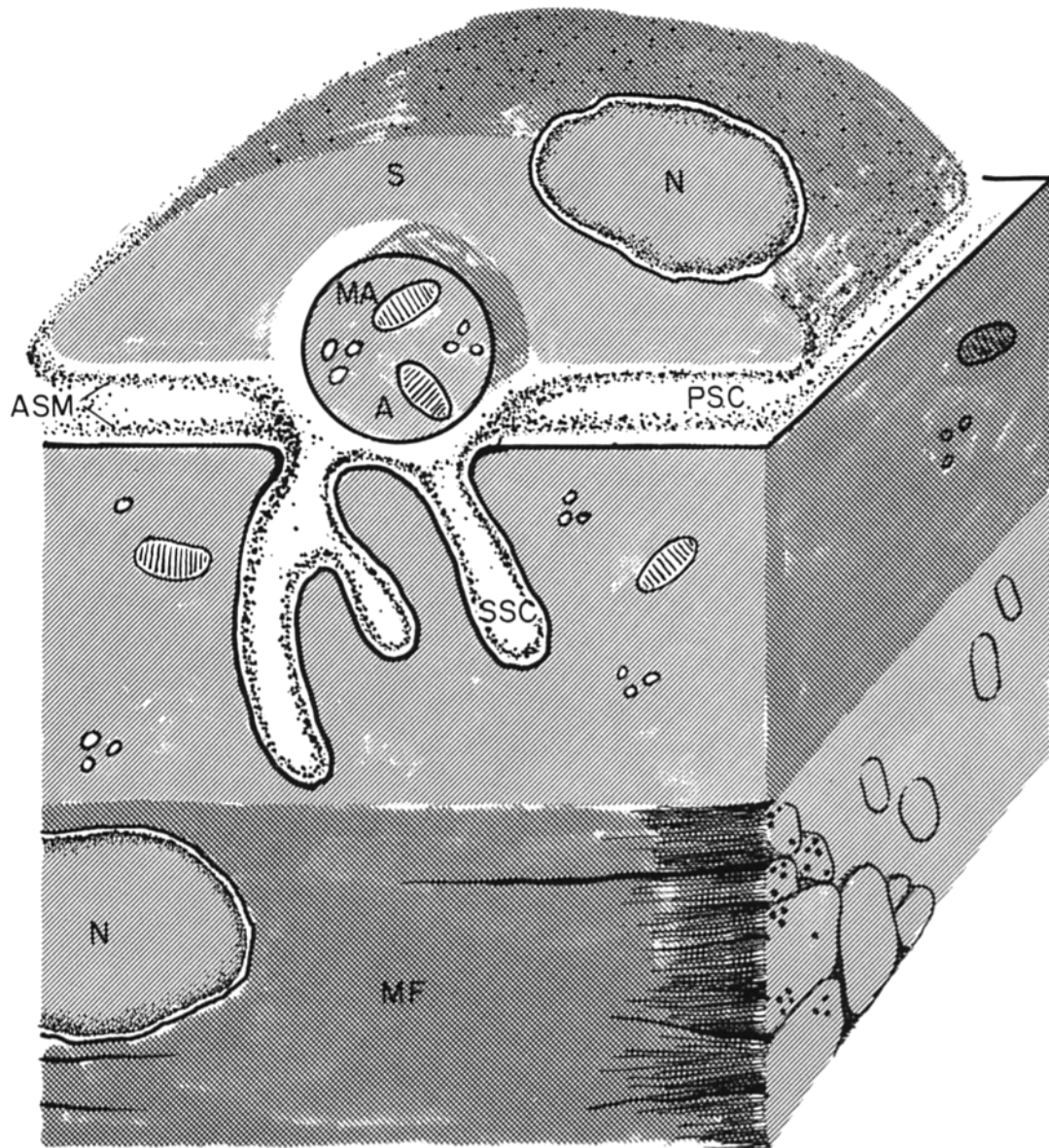

FIGURE 3

Diagram showing the relationships of the ASM within the subsynaptic apparatus.

moderate electron density. Endoplasmic reticulum with granules was frequently noted in the Schwann cell cytoplasm. The axoplasm of the terminal axon branches contained moderate numbers of mitochondria, approximately $0.2 \times 1 \mu$, that were filled with transverse cristae. The axoplasm in well fixed preparations was finely granular and contained variable numbers of round or oval profiles of "synaptic vesicles" (14). The vesicles, which measured approximately 300 A in diameter, were usually most prominent on the axoplasmic surface overlying the sarcolemma.

The nomenclature established by usage will be employed to describe the details of the neuromuscular synapse. The "primary synaptic cleft" is the space lying between the axon membrane and the muscle surface membrane. Subdivisions of the primary synaptic cleft termed "secondary synaptic clefts" project deeply (1 to 1. 5 μ) into the modified sarcoplasm of the sole-plate.

Primary synaptic clefts measured 500 to 600 A in width between axon membrane and muscle surface membrane and contained a material, frequently laminated and somewhat granular, that has been called "ground substance" (13) or basement membrane (37). This material consisted of the fused contributions of two separate bands of amorphous surface material (ASM) approximately 200 A wide, i.e. a layer of finely granular ASM that dipped down from the surface of the terminal Schwann cell, and a second layer of ASM which arose from the muscle surface membrane. Fig. 3 illustrates the relationships of the ASM in the subsynaptic apparatus. The diagram shows the ASM located on the outer or intersynaptic aspect of the relatively electron-dense sarcoplasmic membrane within the secondary clefts. The two components of the ASM join at the edge of the primary synaptic cleft, forming a V-shaped configuration with the apex pointing toward the terminal axon branch in the innervation site. Occasionally two bands of ASM separated by a zone of decreased electron density could be seen within the primary synaptic cleft of human neuromuscular junctions as described by Bickerstaff et al. (3). The ASM within the secondary synaptic clefts was much less prominent in mouse neuromuscular junctions than it was in human junctions.

The secondary synaptic clefts arise as downward invaginations from the primary cleft and penetrate 1.0 to 0.5 μ into the sole-plate region.
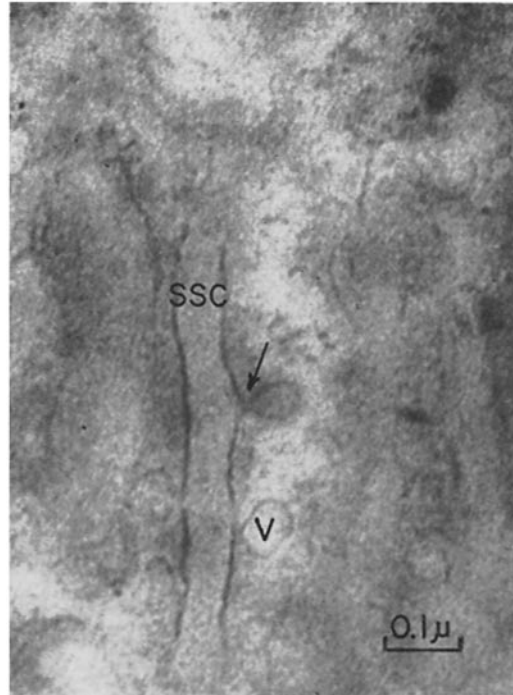

FIGURE 4

Electron micrograph of mouse intercostal neuromuscular junction showing large membrane-limited vesicles in the sarcoplasm adjacent to a secondary synaptic cleft. Continuity between the cleft and the vesicle is evident at the arrow. Methacrylate embedded. $\times$ 100,000.

The neck of each cleft is appreciably narrower (500 A) than the more distal portion (700 to 900 A) (37).

Below the neck portion, the secondary cleft was wider and the dense muscle surface membrane was thinned. Within the secondary clefts were projections of the ASM that were continuous with the bands observed in the primary synaptic clefts. In many micrographs, bands of the ASM appeared to join in the neck region and separate deep within the clefts to form two distinct bands (150 to 200 A) separated by an area of decreased electron density. Similarly, a less electron-dense area was noted between the finely granular bands and the dense muscle surface membrane, similar to that described by Robertson (36) and Reger (34).

The secondary synaptic clefts frequently extended to the myofilaments or were closely related to the outer membrane of the sole-plate nuclei.

Thus, the subneural apparatus consisted of narrow columns of infolded sarcoplasm separated by dense sarcolemma from the layered ASM in the interdigitating secondary clefts. In some micrographs, interruptions approximately 200 to 300 A were noted in the axon membrane which are probably due to oblique sectioning of kinks in the membrane. The sole-plate sarcoplasm showed moderate electron density with rare membrane-limited vesicular structures (650 to 700 A in diameter) within the sarcoplasmic columns.

One micrograph (Fig. 4) shows apparent continuity between one of these vesicles and the lumen of a secondary cleft. This may represent an oblique section through an anastomosis between two secondary clefts (37). Variable numbers of dense aposynaptic granules, 100 to 150 A in diameter, were diffusely scattered or grouped in clusters in the sole-plate area. Moderate numbers of mitochondria with many transverse cristae were scattered in the sole-plate region, and occasional short, straight, or coiled pairs of electron-dense smooth membranes (Fig. 2), 70 to 80 A in width, were randomly found in the sole-plate area.

Human Intercostal Muscle Neuromuscular Junctions: In the course of this investigation, neuromuscular junctions in muscle biopsies from three adults and one child with heart disease have been examined. Observations on the structure of neuromuscular junctions from patients with myasthenia gravis disease is reported elsewhere (43).

The structure of the human intercostal motor end-plate was strikingly similar to that of the mouse (Fig. 5). The innervation site consisted of terminal axon branches lying in synaptic grooves that were subdivided into primary and secondary synaptic clefts. The primary cleft measured 500 to 600 A in width. The secondary synaptic clefts were approximately 400 to 500 A wide at the proximal portion and showed a distal area of widening (700 to 800 A) similar to that seen in the mouse secondary synaptic clefts. Many micrographs showed that the denser portion of the

FIGURE 5

Electron micrograph of neuromuscular junction from human intercostal muscle showing relationships of the Schwann cell, axon, and modified sarcoplasmic surface. The ASM within the synaptic clefts is especially prominent. Methacrylate embedded. × 34,000.

sarcolemma extended for a greater distance into the secondary clefts than in the mouse neuromuscular junction. The relationship of the Schwann cell to the terminal axon and the innervation site was similar to that seen in the mouse neuromuscular junction. The axoplasmic mitochondria measured approximately $0.2 \times 1\,\mu$ and were filled with many transverse cristae. The sarcoplasmic mitochondria measured approximately $0.2 \times 1.2\,\mu$. The primary and secondary synaptic clefts contained discrete bands approximately 200 A wide of moderately electron-dense ASM (Fig. 5), which was considerably more prominent than the ASM seen in the mouse subsynaptic apparatus. The ASM covering the dense sarcolemmal membrane measured up to 300 A in thickness and extended for several millimicrons beyond the area of the secondary synaptic clefts and the surface of the Schwann cell in contact with the axon terminal.

As in the mouse neuromuscular junction, the ASM was continuous with the extracellular connective tissue ground substance and was composed of two joined layers of ASM con-tributed by bands of amorphous material arising on the surfaces of the overlying Schwann cell and the adjacent sarcolemma (Fig. 6).

Definite bands of the ASM ($\sim$200 A wide) separated by a less electron-dense central area were seen in biopsied human muscle, whether embedded in methacrylate or in Epon 812. Narrow zones of less electron-dense material lay between the denser bands of the ASM and the dense sarcolemmic membrane within the secondary clefts. The marked vacuolated appearance of the interdigitating sarcoplasmic columns described by de Harven and Coërs (13) was never observed in well fixed material. Clusters of aposynaptic granules, 100 A in diameter, were scattered in the sole-plate area.

Cytochemical Observations

Lead Staining: When mouse intercostal muscle was stained with high concentrations (50 mg/ml) of Pb $(NO_3)_2$ as in the method of Savay and Csillik (38) and examined by light microscopy, dense particles of PbS were observed outlining occasional end-plates.

Electron micrographs of mouse intercostal neuromuscular junctions stained with 50 mg/ml $Pb(NO_3)_2$ without prior formaldehyde fixation showed electron-dense deposits, primarily in the
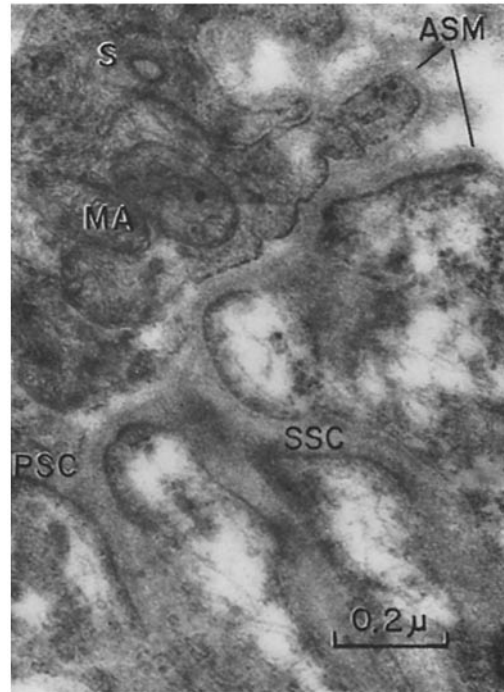

FIGURE 6

Electron micrograph of a human intercostal neuromuscular junction showing the relationship of the two layers of ASM. Note that the ASM extends over the Schwann cell surface membrane and over the muscle surface membrane but does not appear between the Schwann cell and the axon. Methacrylate embedded. $\times$ 75,000.

sarcoplasmic columns of the subsynaptic apparatus. The sarcolemma and myofilaments appeared unusually electron-dense under these conditions of lead staining, whereas the primary and secondary synaptic clefts were unstained (Fig. 7). The results were in general similar to those obtained with lead acetate staining of membranes in tissues other than neuromuscular junctions (40).

PAS Staining: Examination of formalin-fixed, paraffin-embedded, and serially sectioned (6 μ) mouse and human muscle sections showed PAS-positive material in several structures after diastase digestion. Small nerve fibers, observed in longitudinal and transverse section, showed staining of the axon branches and the epineurium. Staining of minute terminal axon branches in end-plate–rich areas was also observed. Muscle cross-striations and capillaries were also stained. Whole mounts stained by PAS after diastase digestion showed marked PAS staining in the fine nerve branches.
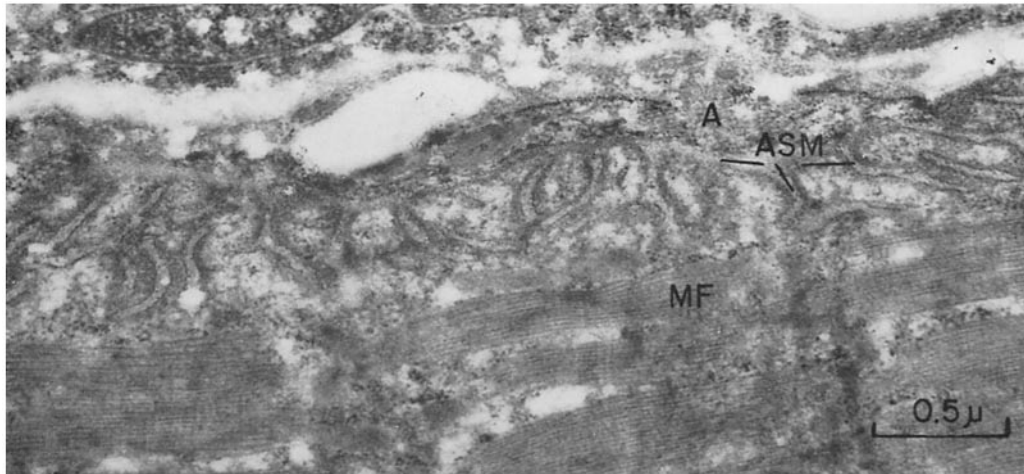
Electron micrograph of a mouse neuromuscular junction after staining with Pb(NO₃)₂. The ASM within the secondary synaptic clefts shows normal electron density, whereas the sarcoplasm and myofilaments show increased electron density. Methacrylate embedded. × 35,000.
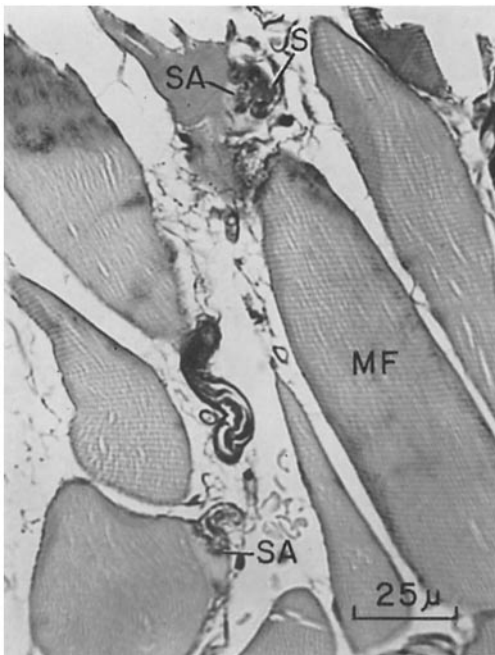

FIGURE 8

Photomicrograph of human intercostal muscle showing PAS-positive subneural apparatus after diastase digestion (methacrylate embedded 2 μ section). × 540.

In 0.5 to 2 μ methacrylate-embedded sections, PAS staining was observed in the capillary walls, in muscle striations, and associated with small nerve fibers. A thin layer of PAS-positive material was observed coating the surfaces of the Schwann cells and sarcolemma (Figs. 8 and 9). In some areas it was possible to detect PAS staining of neuromuscular junctions. In occasional end-plates, it was possible to resolve PAS-stained "batonets" representing the subneural apparatus. Figs. 8 and 9 show 2 μ methacrylate-embedded sections demonstrating PAS-staining batonets in the region of the subneural apparatus.

Alcian Blue–PAS: Thick (6 μ) paraffin-embedded sections stained by the combined PAS and Alcian blue method showed differential staining of nerve and innervation sites (Fig. 10). Transverse sections of medium-sized nerve bundles showed central PAS-stained axis cylinders surrounded by un-stained rings of myelin. The periphery of each myelin cylinder showed a narrow layer in which both PAS and Alcian blue staining were seen. Each nerve fiber was separated from its neighbors by a field of Alcian blue–positive amorphous material. This region corresponds to the peri-neurium and endoneurium of Key and Retzius (21). The outermost layer of connective tissue surrounding the whole nerve and corresponding
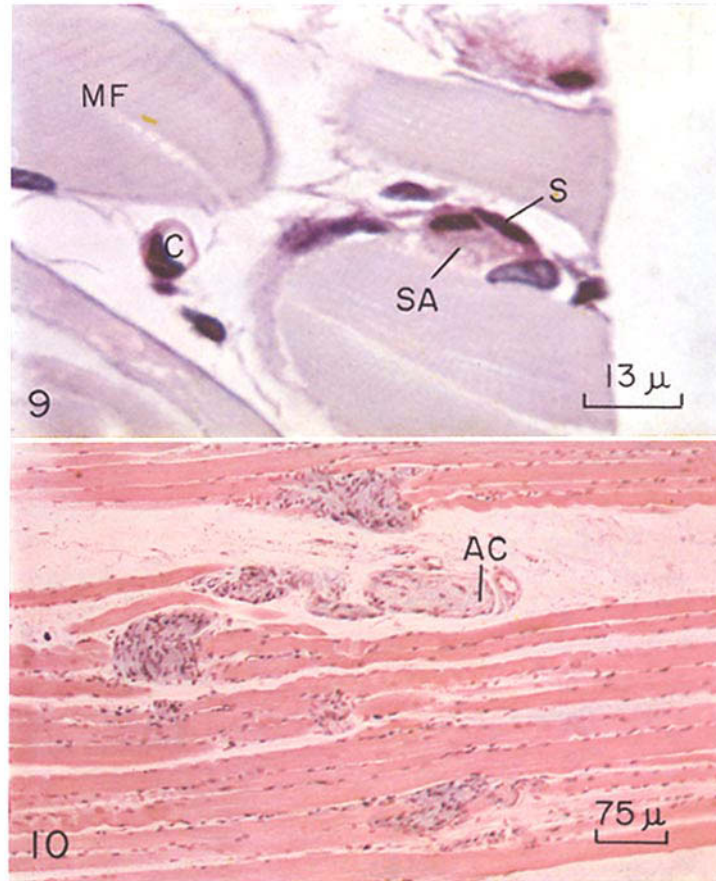
FIGURE 9

Photomicrograph of human intercostal neuromuscular junction (2 μ methacrylate-embedded section) stained by PAS after diastase digestion. Note PAS staining in the region of the subneural apparatus. The horizontal line represents 13 μ. × 1,000.

FIGURE 10

Photomicrograph of human temporal muscle (6 μ paraffin section) stained by the PAS-Alcian blue method. PAS-positive staining is present in axis cylinders and Alcian blue staining in the region of the endoneurium. × 186.

to the epineurium was PAS positive. In regions identified as neuromuscular junctions by the numerous sole-plate nuclei and detail visible in alternate silver-stained serial sections, Alcian blue-staining material formed an ill defined patch of color that contrasted with the magenta PAS-positive axon filaments and capillaries. Muscle fibers distant from innervation sites were unstained by Alcian blue.

Thin (0.5 to 2 μ) methacrylate-embedded sections stained by the combined PAS and Alcian blue method showed PAS-positive material in capillary walls, cross-striations, and on the surface of Schwann cells. Alcian blue–staining areas were difficult to resolve in the thin sections.

DISCUSSION

Comparison of mouse and human neuromuscular junctions has shown marked similarities. Although variations in size and complexity of the pattern of terminal axon filaments occur in various animals (10), the basic structure is similar when examined by electron microscopy. The minor differences

between mouse and human end-plates observed concern the greater extent of the thickened portion of the sarcolemma within the secondary synaptic clefts in human end-plates as compared with the mouse, and the greater prominence of the ASM within the primary and secondary synaptic clefts.

Whereas much attention has been directed to the possible role of the synaptic vesicles in the synthesis, storage, or release of acetylcholine (14), little interest has focused on the material within the primary and secondary synaptic clefts. Because of its strategic position between the axolemma and the sarcolemma, it is probable that the ASM may play an important role in regulating neuromuscular transmission.

The amorphous material was described in detail by Robertson (36) in chameleon neuromuscular junctions, where it formed distinct layers within the secondary clefts. Reger (34) found similar structural relationships in rat neuromuscular junctions. Andersson-Cedergren (1) and de Harven and Coërs (13), however, found amorphous "ground substance" without further differentiation. Recently, Birks et al. (4) have again demonstrated layered differentiation of the ASM within the primary and secondary synaptic clefts of the frog neuromuscular junction. All of these studies (1, 4, 13, 34, 36) have utilized primary osmium fixation. Studies by Birks et al. (4) demonstrated layered bands with osmium fixation followed by phosphotungstic acid staining. When potassium permanganate fixation was employed, neither myofibrils nor external layers of ASM showed appreciable electron density, whereas the cell membranes, synaptic vesicles, nuclei, and mitochondria showed marked electron density. The present study has confirmed the presence of the bands of ASM within the subsynaptic apparatus of both mouse and human neuromuscular junctions prepared by primary formalin fixation followed by brief postosmication. Furthermore, our observations are consistent with the interpretation of Birks et al. (4) concerning the origin of this material from components contributed by both the Schwann cell and the muscle surface membrane and the apparent continuity of this material with the extracellular ground substance.

Although definite layering of this material was occasionally noted in the primary synaptic clefts and uniformly observed in the secondary synaptic clefts, we cannot be certain that these are preformed structures. It may be that even differing methods of fixation precipitates this material in the form of the characteristic bands, and that shrinkage and deformation artifacts occurring during dehydration and embedding give rise to the alternating zones of high and low electron density (37). The ASM retains its relationships in muscle embedded in Epon 812, where shrinkage is less marked than in methacrylate-embedded tissue (17). Attempts to determine the nature of the ASM have been only partially successful. Lead is not preferentially bound by this material under the conditions of staining employed. Previous reports of PAS-staining substances in nerve (9, 18, 23, 26) and in the region of neuromuscular junctions (26) were of interest because of the apparent continuity of the ASM with the extracellular ground substance. McManus et al. (26) reported PAS positivity of nerve and innervation sites in fresh-frozen sections, and Chu (9) showed Schiff-positive material in fresh muscle and brain sections. Chu (9) concluded that the Schiff-positive substances were unsaturated fatty acids derived from lecithin. However, since the PAS-positive material failed to stain after alcohol extraction, it is unlikely that this substance is responsible for PAS reactivity in the paraffin- and methacrylate-embedded sections studied in the present investigation. Similarly, McManus et al. (26) observed that paraffin embedding removed the selective staining of nerve by PAS. It appears that there are extractable substances in fresh or frozen nerve tissue capable of recolorizing the Schiff reagent and that prior oxidation is required to obtain staining after formalin fixation and paraffin embedding.

Recently, Goldstein (18) found diastase-resistant, PAS-positive material outlining striated and cardiac muscle fibers, intercalated discs, and Z bands in several animal species. Alcian blue staining demonstrated the same sites. In the present investigations, PAS-positive material was found on the surfaces of Schwann cells and muscle fibers in cross-striations and in the region of the subsynaptic apparatus.

Both PAS- and Alcian blue–positive material was found intimately related to sites of innervation. Although it was difficult to resolve the batonets of Couteaux in PAS-stained 0.5 to 2 μ methacrylate-embedded sections, several preparations demonstrated that the subneural apparatus

was indeed PAS positive. Supporting this view is the presence of PAS-positive material on the surface of Schwann cells in the region occupied by the ASM, and the PAS-positive material on the surface of the muscle fibers in the region of the second component of the ASM found in the subsynaptic apparatus. Since myelin does not accompany the terminal axon filaments into the primary synaptic clefts, the PAS-positive material observed beneath the Schwann cells in these sections could not be myelin. Furthermore, the axoplasm, which is PAS negative, could not be the source of the staining observed. Thus it is suggested that the finely granular ASM in the subsynaptic apparatus is PAS positive, with an Alcian blue–positive component probably contributed by the terminal Schwann cell. The Alcian blue staining observed in the endoneurium of peripheral nerves is probably due to staining of Schwann cell cytoplasm, since Causey (7) has demonstrated the almost complete absence of fibrocytes in the perineurium and endoneurium.

Numerous substances (32), including polysaccharides, mucopolysaccharides, mucoproteins, glycoproteins, and glycolipids may stain with PAS after diastase digestion. Although PAS staining after disatase digestion is not specific for carbohydrates, the mixed staining with Alcian blue of innervation sites suggests that the material associated with the terminal nerve filaments is at least partially carbohydrate in nature. This is consistent with the suggestion of Robertson (37) that the "basement membrane" is a highly hydrated mucopolysaccharide or mucoprotein.

Of interest in this connection is the observation that curare is bound to a carbohydrate in extracts of electric organ (8) and that receptor material isolated from the electric eel contains carbohydrate (15). Furthermore, acetylcholinesterase, which may be chemically similar to serum cholinesterase, a glycoprotein (2), is found in the primary and secondary synaptic clefts (22, 41).

The presence of the ASM, either amorphous or layered, between the axolemma and the sarcolemma should have important consequences for theories of neuromuscular transmission because neurohumoral transmitters or substances that affect neuromuscular transmission must traverse this potential barrier. Intercellular material is also found in central nervous system synapses (30), and molluscan cardiac muscle cells, which are extremely sensitive to acetylcholine (20, 33), are

coated by similar, though less electron-dense, amorphous material that is Alcian blue and PAS positive (42). Although the term "basement membrane" has been avoided in the present description of the amorphous material (ASM) outside the plasma membrane of the Schwann cell because of possible confusion with terminology borrowed from histology (where it would be inappropriate), it has been applied by electron microscopists to amorphous material occurring in this location (7) and in other sites (6, 16, 31).

The ASM is structurally similar to the "basement membrane" of the renal glomerulus (16), duodenal epithelium (31), and epididymis (6). A common feature of these absorptive cells is the necessity for ions and macromolecules to traverse the "basement membrane" before entering the cell. It is possible that the "basement membrane" of the neuromuscular junction, which extends into the complex ramifications of the subsynaptic apparatus, may have a similar function.

It is premature to speculate in detail on the physiologic role of the ASM in neuromuscular transmission. In the original theory of Dale (11), acetylcholine, a neurohormone, is liberated by the axon terminal, traverses the synaptic interface, and excites the postsynaptic membrane. Nachmansohn (28) believes that the "complete system is present on both sides of the intercellular gap, in the membrane of the nerve terminal and in the postsynaptic membrane." In one theory, the basement membrane between the axolemma and the sarcolemma might act as an organized system to facilitate ion transfer, whereas in the other theory it might serve as a potential barrier.

Neuromuscular junction degeneration following nerve section produces no visible anatomic changes in the basement membrane layers (5, 35), and there appear to be occasional abnormalities in this material in neuromuscular junctions from patients with myasthenia gravis (43). A recent investigation (44) of the localization of ferritin-labeled botulinus B toxin in the mouse neuromuscular junction has shown that the toxin is localized in the ASM of the Schwann cells and within the primary and secondary synaptic clefts.

BIBLIOGRAPHY

1. Andersson-Cedergren, E. A., *J. Ultrastruct. Research*, 1959, suppl. 1, 1.
2. Bader, R., Schultz, F., and Stacey, M., *Nature*, 1944, **154**, 183.
3. Bickerstaff, E. R., Evans, J. V., and Woolf, A. L., *Nature*, 1959, **184**, 1500.
4. Birks, R., Huxley, H. E., and Katz, B., *J. Physiol.*, 1960, **150**, 134.
5. Birks, R., Katz, B., and Miledi, R., *J. Physiol.*, 1960, **150**, 145.
6. Burgos, M., Symposium on Fine Structure, International Congress of Anatomy, New York, 1960.
7. Causey, G., The Cell of Schwann, London, E. & S. Livingstone, Ltd., 1960.
8. Chagas, C., *Ann. New York Acad. Sc.*, 1959, **81**, 345.
9. Chu, C. H. U., *Anat. Rec.*, 1950, **108**, 723.
10. Cole, W. V., *J. Comp. Neurol.*, 1955, **102**, 671.
11. Dale, H. H., *Proc. Mayo Clin.*, 1955, **30**, 5.
12. Davis, B. J., Ornstein, L., Taleporos, P., and Koulish, S., *J. Histochem. and Cytochem.*, 1959, **7**, 291.
13. De Harven, E., and Coërs, C., *J. Biophysic. and Biochem. Cytol.*, 1959, **6**, 7.
14. De Robertis, E. D. P., and Bennett, H. S., *J. Biophysic. and Biochem. Cytol.*, 1955, **1**, 47.
15. Ehrenpreis, S., *Biochim. et Biophysica Acta*, 1960, **44**, 561.
16. Farquhar, M. G., Vernier, R. L., and Good, R. A., *J. Exp. Med.*, 1957, **106**, 649.
17. Finck, H., *J. Biophysic. and Biochem. Cytol.*, 1960, **7**, 27.
18. Goldstein, D. J., *Anat. Rec.*, 1959, **134**, 217.
19. Gridley, M. F., Manual of Histologic and Special Staining Technics, Washington, D. C., Armed Forces Institute of Pathology, 1957.
20. Jullien, A., and Vincent, D., *Compt. rend. Acad. sc.*, 1938, **206**, 209.
21. Key, A., and Retzius, G., *Arch. mikr. Anat.*, 1873, **9**, 308.
22. Lehrer, G. M., and Ornstein, L. A., *J. Biophysic. and Biochem. Cytol.*, 1959, **6**, 399.
23. Liang, H. M., *Anat. Rec.*, 1947, **99**, 511.

24. Luft, J., cited by Pease, D. C., Histological Techniques for Electron Microscopy, New York, Academic Press, Inc., 1960, 84.
25. McManus, J. F. A., *Stain Techn.*, 1948, **23**, 99.
26. McManus, J. F. A., Saunders, J. C., Penton, G. B., and Cason, J. E., *Science*, 1950, **111**, 155.
27. Mowry, R. W., and Morard, J. C., *Am. J. Path.*, 1957, **33**, 620.
28. Nachmansohn, D., Chemical and Molecular Basis of Nerve Activity, New York, Academic Press, Inc., 1959.
29. Ornstein, L., and Pollister, A. W., *Trans. New York Acad. Sc.*, Series II, 1952, **14**, 194.
30. Palay, S. L., *Exp. Cell Research*, 1958, suppl. **5**, 275.
31. Palay, S. L., *J. Biophysic. and Biochem. Cytol.*, 1959, **5**, 363.
32. Pearse, A. G. E., Histochemistry, Boston, Little, Brown & Company, 1954.
33. Pilgrim, R. L. C., *J. Physiol.*, 1954, **125**, 208.
34. Reger, J. F., *Anat. Rec.*, 1958, **130**, 7.
35. Reger, J. F., *J. Ultrastruct. Research*, 1959, **2**, 269.
36. Robertson, J. D. *J. Biophysic. and Biochem. Cytol.*, 1956, **2**, 381.
37. Robertson, J. D., *Am. J. Physical Med.*, 1960, **39**, 1.
38. Savay, G. Y., and Csillik, B., *Nature*, 1958, **181**, 1137.
39. Ward, R. D., *J. Histochem. and Cytochem.*, 1958, **6**, 398.
40. Watson, M. L., *J. Biophysic. and Biochem. Cytol.*, 1958, **4**, 475.
41. Zacks, S. I., and Blumberg, J. M., *J. Histochem. and Cytochem.*, 1961, **9**, 317.
42. Zacks, S. I., and Blumberg, J. M., unpublished observations.
43. Zacks, S. I., Bauer, W. C., and Blumberg, J. M., *Nature*, 1961, **190**, 280.
44. Zacks, S. I., Metzger, J. M., Smith, C. W., and Blumberg, J. M., Proceedings IV International Congress for Neuropathology, Munich, 1961, in press.